encit 2020

ABCM Associação Brasileira de Engenharia e Ciências Mecânicas

18th Brazilian Congress of Thermal Sciences and Engineering
November 16–20, 2020 (Online)

ENC-2020-0511
NUMERICAL SIMULATION IN SHALLOW WATER AT SANTA BÁRBARA DAM.

Rafael Zanovelo Perin
Régis Sperotto de Quadros
Armando Miguel Awruch
Federal University of Pelotas - Institute of Physics and Mathematics
Pelotas - RS - Brazil
rafael-perin@hotmail.com
quadros99@gmail.com
amawruch@ufrgs.br

Renato Vaz Linn
Federal University of Rio Grande do Sul - Engineering School
Porto Alegre - RS - Brazil
renatolinn@ufrgs.br

Abstract. *Water is fundamental for life and development, attracting the permanence of communities in its surroundings. Use and handling of water resources was encouraged in order to maximize their benefits and possibilities, such as the installation of dams. However, several dangers, such as floods provoked by dams rupture and water pollution with its undesirable consequences, arise simultaneously becoming even more serious due to urbanization. For the development of studies related to disasters provoked by a dam rupture, it is necessary to know the water flow in these artificial barriers. A mathematical model using the shallow water equations applied to Santa Bárbara Dam, located in Pelotas City (in the southern region of Brazil) is proposed in this work. The numerical simulation of the model is performed by applying the finite element method (FEM) together with the characteristic-based split (CBS) method for space and time discretization, respectively.*

Keywords: *finite element method, characteristic-based split method, shallow water equations, Santa Bárbara Dam, Pelotas City.*

1. INTRODUCTION

Since the beginning of civilizations, water has been a natural resource of reference for the development, attracting people and encouraging progress in their surroundings (Cardoso, 1980). This was due to the fact that water resources satisfy different human needs, such as hydration, food, agriculture, transport, energy generation, among others.

From the dependence and presence of water, considering that 70% of the surface of our planet is composed of water, civilizations were subjected to environment adversities, whether in the form of floods, water scarcity, organic material pollution and other ecological disasters. Thus, it has become essential to control water resources in order to minimize human and economic damages.

Dams construction took place with the purpose of retaining and controlling water, aiming to minimize the impacts of scarcity. Over time, the use of these artificial barriers has been extended, encompassing energy production and promoting agricultural development in its surroundings. On the other side, a dam has several negative impacts on the environment because they are harmful to the aquatic fauna, in addition to the possibility of breaking, which would cause floods with their harmful consequences.

With the installation of cities in the vicinity of water sources (lakes, rivers, seas, etc.), it is necessary to know the behavior of water bodies and to predict the scope of possible environmental disasters, especially in the case of dams rupture and the ensuing floods caused by this event. Therefore, the control of the water level in this type of artificial barrier is essential in preventing accidents. Therefore, the use of hydrodynamic models was promoted in the forecast and understanding of these flows (Grave, 2016).

A mathematical model using the shallow water equations at Santa Bárbara Dam, located in the Pelotas city, in the southern part of Brazil, as a case study, is proposed in this work. The numerical simulation is carried out with a hydrodynamic model discretized in time by the characteristic-based split method (CBS), while in space the finite element method

(FEM) is adopted. The dam mesh is obtained using triangular elements and linear interpolation functions and employing a totally explicit scheme, obtaining a flow forecast in order to represent possible floods.

2. SHALLOW WATER EQUATIONS

Shallow water equations come from the integration of continuity and momentum equations along the depth, applying the Leibniz rule for variable contour integrals (Awruch, 1983).

The equations describing a two-dimensional incompressible flow with a free surface are obtained adopting the following hypotheses: the specific mass (ρ) is constant, the horizontal dimensions are much higher than the vertical dimension, the pressure (p) has an hydrostatically behaviour, the bottom topography is time independent, the vertical velocity component is very small and its acceleration is neglected, the velocity components at the bottom are zero and the horizontal velocity components are not uniform, but for convenience, they are taken as having constant values in with depth direction ($\hat{U}_i(x_1, x_2, t)$) (Zienkiewicz *et al.*, 2005).

The system of shallow water equations is given by:

$$\frac{\partial h}{\partial t} + \frac{\partial U_i}{\partial x_i} = 0, \tag{1}$$

$$\frac{\partial U_i}{\partial t} + \frac{\partial F_{ij}}{\partial x_j} + \frac{g}{2}\frac{\partial \eta}{\partial x_i}\frac{\partial H}{\partial x_i} - \frac{\partial}{\partial x_j}\left[\chi\left(\frac{\partial U_i}{\partial x_j} + \frac{\partial U_j}{\partial x_i}\right)\right] + (-1)^i \nu U_k + \left(\frac{g}{c_m^2}\frac{|U|}{h^2}U_i\right) = \overline{c_d}|W|W_i, \tag{2}$$

in the domain Ω with $i, j = 1, 2$ and $k = i + (-1)^{i+1}$, where $u_i(x_1, x_2, t)$ is the component of the instantaneous velocity in the direction x_i, $U_i(x_1, x_2, t)$ is the component of the flow (flow per unit width) in the direction of x_i, $h(x_1, x_2, t)$ is the total depth, $H(x_1, x_2)$ is the distance from the reference plane to the bottom (assumed to be time independent) and $\eta(x_1, x_2, t)$ is the elevation of the free surface in relation to the reference plane. Also, $U_i = \hat{U}_i\, h$, $F_{ij} = \hat{U}_i\, U_j$, $h = H + \eta$, χ is a generalized viscosity coefficient given in m^2/s (usually $\chi = 0$ is adopted), g is the gravity acceleration (m/s^2), $\nu = 2\,\omega\, sin\,\Theta = 1.4.10^{-4}\, sin\,\Theta$ is the Coriolis coefficient (where $\omega = 7.10^{-5}\, rad/s$ is the angular rotation speed for Earth and Θ is the latitude of the point being considered), c_m is the Chezy coefficient (given in $m^{\frac{1}{2}}/s$), which is linked to the Manning coefficient υ by the expression $c_m = h^{\frac{1}{6}}/\upsilon$ (where υ is given in $s/m^{\frac{1}{3}}$ and g/c_m^2 is dimensionless), $\overline{c_d}$ is a dimensionless drag coefficient, $|W|W_1 = |W||W|cos\vartheta$ e $|W|W_2 = |W||W|sin\vartheta$, where $|W|$ is the absolute value of the wind speed and ϑ is the wind direction (Bukatov and Zav'yalov, 2004).

Shallow water systems are characterized by long the wavelengths, where the wave speed c_w is given by:

$$c_w \cong \sqrt{gh}; \qquad c_w^2 = \frac{dp}{dh} = \frac{1}{c_w^2}\frac{\partial p}{\partial t}, \tag{3}$$

being the pressure given by:

$$p = \frac{1}{2}g(h^2 - H^2). \tag{4}$$

2.1 Boundary Conditions

The initial and boundary conditions must be given to the governing equations. Initial conditions values of U and h in $t = 0\ s$ must be provided. The forced boundary conditions, of Dirichlet type, are:

a) $\mathbf{U} \cdot \mathbf{n} = U_i n_i = 0$ inΓ_w("solid" or "closed" boundary);

b) $\mathbf{U} \cdot \mathbf{n} = U_i n_i = \overline{U}_n$ inΓ_U("fluid" or "open" boundary);

c) $h = \overline{h}$ inΓ_h("fluid" or "open" boundary).

$\overline{U}_n$ and $\overline{h}$ are prescribed values for the unknowns in the Γ_U and Γ_h parts of the total boundary Γ, being n_i the unitary vector normal to boundaries Γ_W and Γ_U. The total boundary Γ is the union of each one of the parts, that is, $\Gamma = \Gamma_w \cup \Gamma_U \cup \Gamma_h$.

3. NUMERICAL MODEL AND DISCRETIZATION

Spatial discretization of the equations is using the Finite Element Method (FEM), employing triangular elements with linear interpolation functions. For temporal discretization the Characteristic-Based Split (CBS) method is used, being this scheme an useful technique for advection dominated problems.

FEM is a technique by which a continuous problem is transformed into a discrete one, so that the solution is obtained in a finite number of point (element nodes).

A generic triangular finite element is shown in Fig. 1, with its nodes (1, 2 and 3) and respective coordinates (x_i, y_i).

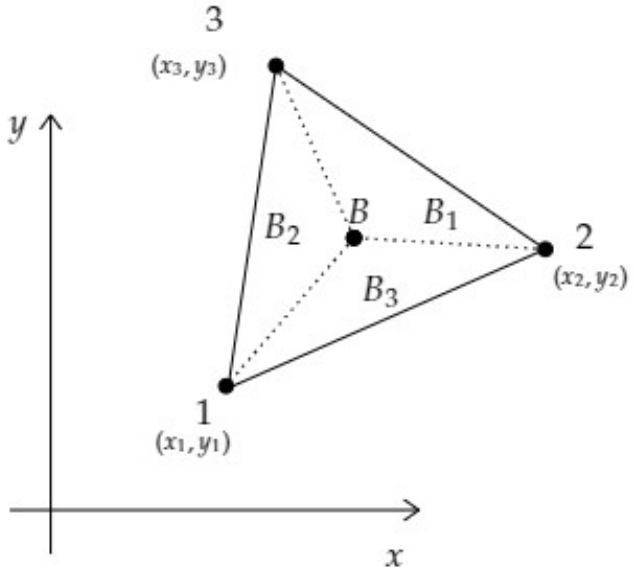

Figure 1. Triangular finite element with three nodes.

Any point B located inside the element, with coordinates x and y allows to subdivide the triangle of area A into three triangles of areas B_1, B_2 and B_3, in such a way that they give origin to a new dimensionless coordinate system, called triangular or natural coordinates Huebner *et al.* (2001). These coordinates are related to the cartesian coordinates by:

$$L_i = \frac{(a_i + b_i\ x + c_i\ y)}{2A} \quad (i = 1, 2, 3), \tag{5}$$

$$L_1 + L_2 + L_3 = 1, \tag{6}$$

$$\underline{\phi} = [L_1 \ \ L_2 \ \ L_3], \tag{7}$$

where $\underline{\phi}$ is a vector with the linear element interpolation functions ($\underline{\phi} = [\phi_1 \ \ \phi_2 \ \ \phi_3]$) and:

$$a_i = x_j\ y_k - x_k\ y_j; \quad b_i = y_j - y_k; \qquad c_i = x_k - x_j, \tag{8}$$

when $i = 1$, $j = 2$ and $k = 3$; when $i = 2$, $j = 3$ and $k = 1$; when $i = 3$, $j = 1$ and $k = 2$.

The spatial discretization of the governing equations is perfomed using the classical Bubnov-Galerkin method and calculating integral terms at element level. Thus, the Eq. 1 and 2 can be written as:

$$\underline{M}\ \dot{\underline{h}} + \underline{A}_i\ \underline{U}_i = 0, \tag{9}$$

$$\underline{M}\ \dot{\underline{U}}_i + \underline{K}_i\ \underline{U}_i + \underline{K}_k\ \underline{U}_k + g\ \overline{h}\ \underline{A}_i\ \underline{h} = \underline{P}_i^U, \tag{10}$$

where the "–" symbol below indicates matrices and vectors where as the symbol above the variable indicates the values in the element center. Vectors $\underline{h}$ and $\underline{U}_i$ contain nodal variables of the total depth h and the flow components U_i, respectively. Time derivatives of these variables and the value of the h on the element center are given by:

$$\dot{\underline{h}} = \frac{\partial \underline{h}}{\partial t}, \ \ \dot{\underline{U}_i} = \frac{\partial \underline{U}_i}{\partial t} \quad \text{and } \overline{h} = \underline{\phi}\ \underline{h} = \frac{(h_1 + h_2 + h_3)}{3}. \tag{11}$$

The matrices and vectors due to wind action are given by:

$$\underline{M} = \int_A (\underline{\phi}^T\ \underline{\phi})\ dA \qquad \underline{A}_i = \int_A \left(\underline{\phi}^T\ \frac{\partial \underline{\phi}}{\partial \underline{x}_i}\right)\ dA$$

$$\underline{K}_k = [(-1)^i\ \nu\ \underline{M}] \qquad \underline{P} = \int_A \underline{\phi}^T\ dA$$

$$\underline{K}_i = \left[\underline{A}_j^u + \left(\frac{g}{c_m^2}\right)\left(\frac{|\overline{U}|}{\overline{h}^2}\right)\underline{M}\right] \qquad \underline{A}_j^u = \int_A \left(\underline{\phi}^T\ \frac{\partial \underline{\phi}}{\partial \underline{x}_j}\right)\ \underline{\hat{U}}_j^T\ dA$$

$$\underline{P}_i^U = (\overline{c_d}\ |W|\ W_i)\underline{P} - g\ \overline{h}\ \underline{A}_i\ \underline{H}.$$

For the temporal discretization, the characteristic-based split scheme is applied, which is very useful for advection dominant problems (Zienkiewicz *et al.*, 2005). The procedure consists in the separation of the problem variables (components of the flow per unit width U_i and the total depth h) using three different steps.

The first step of the CBS scheme consists of solving the momentum equation explicitly without pressure terms obtaining ΔU_i^*. In the second step, using ΔU_i^* calculated in the first step, Δp is computed employing also an explicit algorithm. The pressure p is related to the total depth h by the expression $h = [H^2 + \frac{2p}{g}]^{\frac{1}{2}}$. In the third step, using values of Δ_i^* and Δp, obtained previously, $\Delta U_i = \Delta U_i^* + \Delta U_i^{**}$ is computed. Finally, variables U_i and h are obtained.

The stability condition is given by:

$$\Delta t \leq \Delta t_{crit}, \tag{12}$$

where $\Delta t = t^{n+1} + t^n$ is the time interval and Δt_{crit} is the critical time step, which is given by:

$$\Delta t_{crit} = \frac{l}{c_w + |U_i|}, \tag{13}$$

being l a characteristic size of the element, c_w is given by Eq.(3) and $|U_i|$ is the absolute value of U_i (Wijaya *et al.*, 2008).

Following the methodology mentioned above, the steps of the CBS procedure are:

Step 1:

$$(\underline{M}_D \Delta \underline{U}_i^*)^{m+1} = -\Delta t \{ \left[(\underline{A}_j^u + \underline{M}^\beta)\underline{U}_i + \underline{M}^\nu \, \underline{U}_k + \underline{A}_i^H \underline{H} - \underline{P}_i^w \right] +$$

$$-\frac{\Delta t}{2} \left[(-\underline{D}_{kj}^u + \underline{A}_k^{u,\beta})\underline{U}_i + \underline{A}_k^{u,\nu} \, \underline{U}_s - \underline{D}_{ki}^{u,H} \underline{H} - \underline{P}_{k,i}^{u,w} + \underline{f}_{kj}^u \right] \}^n + (\underline{M}_D - \underline{M})(\Delta \underline{U}_i^*)^m; \tag{14}$$

Step 2:

$$\left(\frac{\overline{h}}{c_w^2} \underline{M}_D \Delta \underline{p} \right)^{m+1} = -\Delta t \left\{ \underline{A}_j \left(\underline{U}_j + \frac{1}{2} \Delta \underline{U}_j^* \right) - \frac{\Delta t}{2} \overline{h} (-\underline{D'}_{kj} \underline{p} + \underline{f}_p) \right\}^n + \frac{1}{c_w^2} (\underline{M}_D - \underline{M}) \Delta \underline{p}^m; \tag{15}$$

Step 3:

$$(\underline{M}_D \, \Delta \underline{U}_i)^{m+1} = \underline{M} \, \Delta \underline{U}_i - \Delta t \, \overline{h} \left[\underline{A}_i \, \underline{p} - \frac{\Delta t}{2} (-\underline{D}_{ki}^u \, \underline{p} + \underline{f}_p^u) \right]^n + (\underline{M}_D - \underline{M})(\Delta \underline{U}_i)^m; \tag{16}$$

Final calculations:

$$\underline{U}_i^{n+1} = \underline{U}_i^n + \Delta \underline{U}_i \qquad \underline{p}^{n+1} = \underline{p}^n + \Delta \underline{p}$$

$$\underline{h}^{n+1} = \left[\underline{H}^2 + \frac{2\underline{p}}{g} \right]^{\frac{1}{2}} \qquad \hat{\underline{U}}_i^{n+1} = \frac{\underline{U}_i^{n+1}}{\underline{h}^{n+1}},$$

with $i, j, k = 1, 2$ and $s = i + (-1)^{i+1}$, m being the number of iterations and n the instant of time.

The matrices and vectors are:

$$\underline{M} = \int_\Omega \underline{\phi}^T \, \underline{\phi} \, d\Omega \qquad \underline{M}^\nu = \nu' \, \underline{M} \qquad \underline{M}^\beta = \beta \, \underline{M}$$

$$\underline{M}_D = \tfrac{\Omega}{3} \underline{I} \qquad \underline{A}_j = \int_\Omega \left(\underline{\phi}^T \frac{\partial \underline{\phi}}{\partial \underline{x}_j} \right) d\Omega \qquad \underline{A}_j^u = \int_\Omega \underline{\phi}^T \left(\frac{\partial \underline{\phi}}{\partial \underline{x}_j} \hat{\underline{U}}_j \right) d\Omega$$

$$\underline{A}_k^{u,\beta} = \int_\Omega \underline{\phi}^T \left(\hat{\underline{U}}_k \frac{\partial \underline{\phi}}{\partial \underline{x}_k} \right) d\Omega \quad \underline{A}_k^{u,\nu} = \nu' \int_\Omega \underline{\phi}^T \left(\hat{\underline{U}}_k \frac{\partial \underline{\phi}}{\partial \underline{x}_k} \right) d\Omega \qquad \underline{A}_i^H = g \, \underline{\eta} \int_\Omega (\underline{\phi}^T \frac{\partial \underline{\phi}}{\partial \underline{x}_i}) d\Omega$$

$$\underline{P}_i^w = \gamma_i \int_\Omega \underline{\phi}^T d\Omega \qquad \underline{P'}_k = \int_\Omega \frac{\partial \underline{\phi}^T}{\partial \underline{x}_k} d\Omega \qquad \underline{P}_{k,i}^{u,w} = \gamma_i \int_\Omega \frac{\partial (\hat{\underline{U}}_k \underline{\phi}^T)}{\partial \underline{x}_k} d\Omega$$

$$\underline{D}_{kj}^{'} = \int_\Omega \frac{\partial \underline{\phi}^T}{\partial \underline{x}_k} \frac{\partial \underline{\phi}}{\partial \underline{x}_j} \qquad \underline{D}_{kj}^u = \int_\Omega \frac{\partial (\hat{\underline{U}}_k \underline{\phi}^T)}{\partial \underline{x}_k} \frac{\partial (\hat{\underline{U}}_j \underline{\phi})}{\partial \underline{x}_j} d\Omega \qquad \underline{D}_{ki}^{u,H} = g \, \eta \int_\Omega \frac{\partial (\hat{\underline{U}}_k \underline{\phi}^T)}{\partial \underline{x}_k} \frac{\partial \underline{\phi}}{\partial \underline{x}_i}$$

$$\underline{f} = \int_\Gamma \underline{\phi}^T \, q_n^p d\Gamma \qquad \gamma_i = \overline{c_d} \, |W| \, W_i \qquad \beta = \frac{g \, |\underline{U}|}{c_m^2 \, \overline{h}^2}$$

$$\underline{f}_{kj}^u = \int_\Gamma (\hat{\underline{U}}_k \underline{\phi}^T) \frac{\partial (\hat{\underline{U}}_j \phi)}{\partial \underline{x}_j} n_j \, d\Gamma = \int_\Gamma (\hat{\underline{U}}_k \underline{\phi}^T) q_n^u d\Gamma$$

$$\underline{f}_p^u = \int_\Gamma (\hat{\underline{U}}_k \underline{\phi}^T) \frac{\partial (\phi p)}{\partial \underline{x}_j} n_j \, d\Gamma = \int_\Gamma (\hat{\underline{U}}_k \underline{\phi}^T) q_n^p d\Gamma$$

$$q_n^u = \frac{\partial(\phi\ \hat{\underline{U}}_j)}{\partial x_j} n_j = \frac{\partial(\hat{U}_j)}{\partial x_j} n_j \qquad q_n^p = \frac{\partial p}{\partial x_n} = \left[\frac{\partial(\phi\ p)}{\partial x_j}\right] n_j$$

$$\underline{D}_{kj}^u(m,n) = \underline{D}_{kj}^{'}[(m),(n)]\underline{\hat{U}}_k[(m)]\underline{\hat{U}}_j[(n)] \qquad \underline{P}_{k,i}^{u,w}(n) = \underline{P}_k^{'}[(n)]\underline{U}_k[(n)]$$

$$\underline{A}_k^{u,\beta}(m,n) = \beta\ \underline{\hat{U}}_k[(n)]\underline{A}_k[m,(n)] \qquad \underline{A}_k^{u,\nu}(m,n) = \overline{\nu}\ \underline{\hat{U}}_k[(n)]\underline{A}_k[m,(n)]$$

where I is the 3x3 identity matrix, $\nu' = (-1)^i\ \nu$, $\overline{\eta} = \overline{h} - \overline{H}$ and $i, j, k = 1, 2$.

Vectors generated by the CBS scheme must be assembled for all the elements of the finite element mesh.

4. STUDY CASE

The Santa Bárbara Dam was built in Pelotas city, located as Fig. 2 in the state of Rio Grande do Sul (RS), Brazil (latitude: $-31°46'19"$; longitude: $-52°20'33''$) (Lima, 2016). The purpose of the construction was to prevent flooding in the urban area and to supply the population with drinking water, with an accumulation basin 3 to 4 meters deep and a capacity of 10 million cubic meters approximately (SANEP, 2020).

The municipality has recurrent floods caused by meteorological phenomena, causing inconvenience to the population. Due to the location of the dam in the urban area, its surroundings are inhabited, so that floods and disruptions can be quite worrying and impactful in the region. For this reason, hydrodynamic studies become relevant at this location.

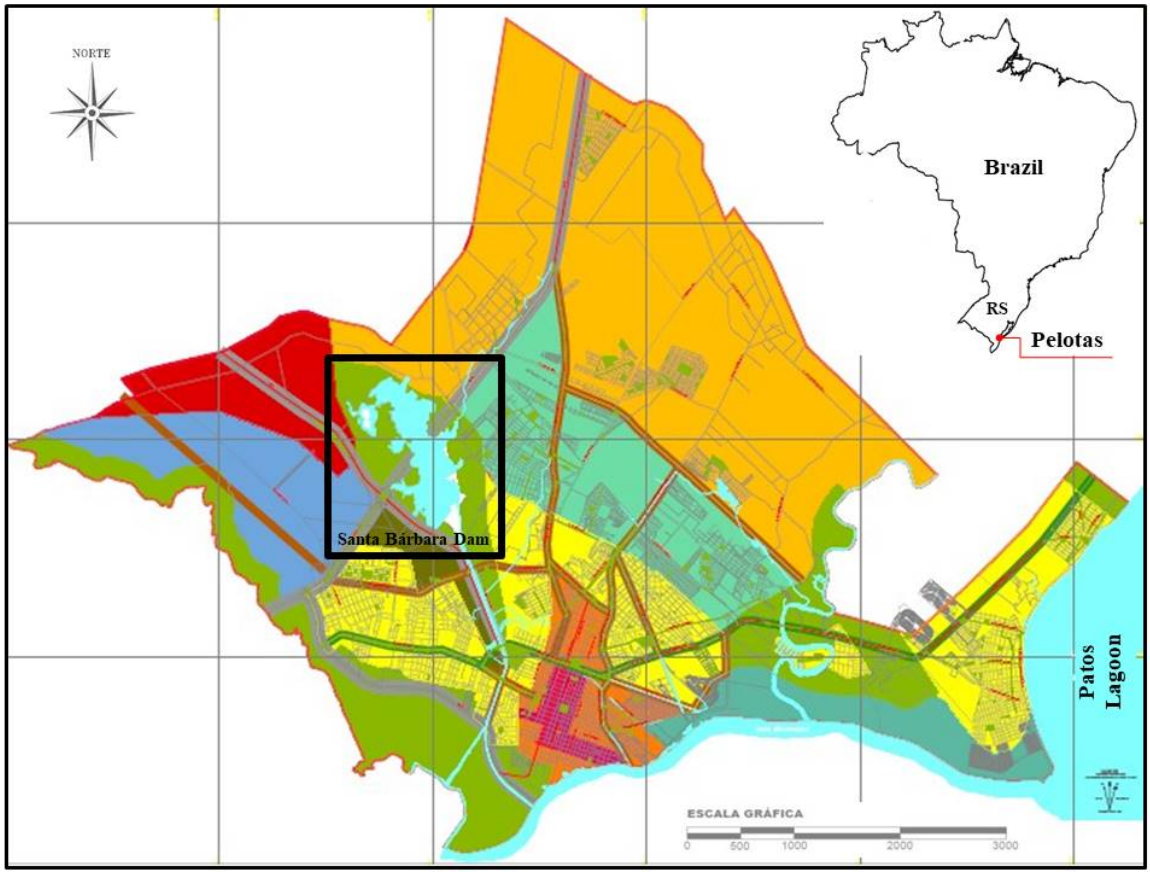

Figure 2. Location of Pelotas (urban area).

The methodology was implemented in FORTRAN language and validated by Grave (2016) for numerical simulation in shallow water, with the effects of wind and Coriolis being added. With the reproduction of the dam in the AutoCAD software (Pelotas, 2016), GiD software was used for the development of the finite element computational mesh, Fig. 3, with 27,382 nodes and 52,195 triangular elements. Also, in the computational mesh, the red boundary are highlighted, for output marked C and for input D, E and F. While, the rest of the contour is solid.

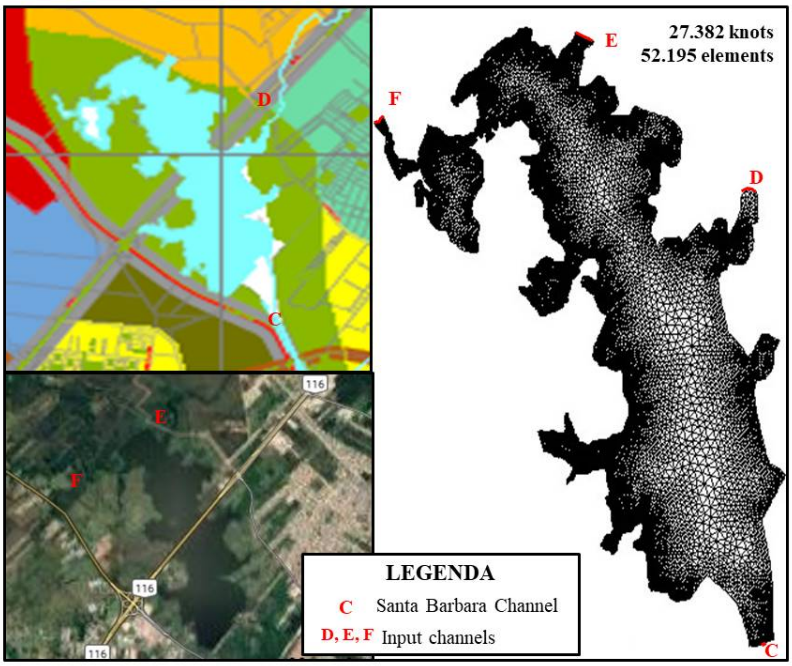

Figure 3. Santa Bárbara Dam: a) map location; b) mesh in triangular elements.

5. Results

Numerical simulation was carried out in shallow water applied to Santa Bárbara Dam, for that, some parameters from the literature were used according to the object of study. So, for simulations $\upsilon = 0.020$ was used due to the bottom being composed mostly of sand (Coon, 1998), $\Theta = -31°$ of city latitude (Lima, 2016), $\vartheta = 179°$ e $W = 3.93\ m/s$ due to the arithmetic mean of the directions and maximum gusts for October 9, 2020 (WINDFINDER, 2020), $\overline{c_d} = 3.2.10^{-6}$ for drag (Gill, 1982) and prescribed inflows in Γ_U. The initial conditions used were $U_i(x_1, x_2, 0) = 0\ m^2/s$ and $h(x_1, x_2, 0) = 3.8\ m$.

In Fig. 4, at $t = 150\ s$ there is a predominance of $h(x_1, x_2, 0)$, represented in the transition between green and yellow on the scale, with emphasis on the first. The largest variations in the water level are found in the surrounding of the entry and exit contours Γ_U, being above and below the initial height, respectively. At $t = 1,800\ s$ the total height of the water rises in the upper part of the water resource, especially where the geometry is more complex, while next to the flow there is a reduction in the level, still in green, and more concentrated in the Santa Bárbara Channel.

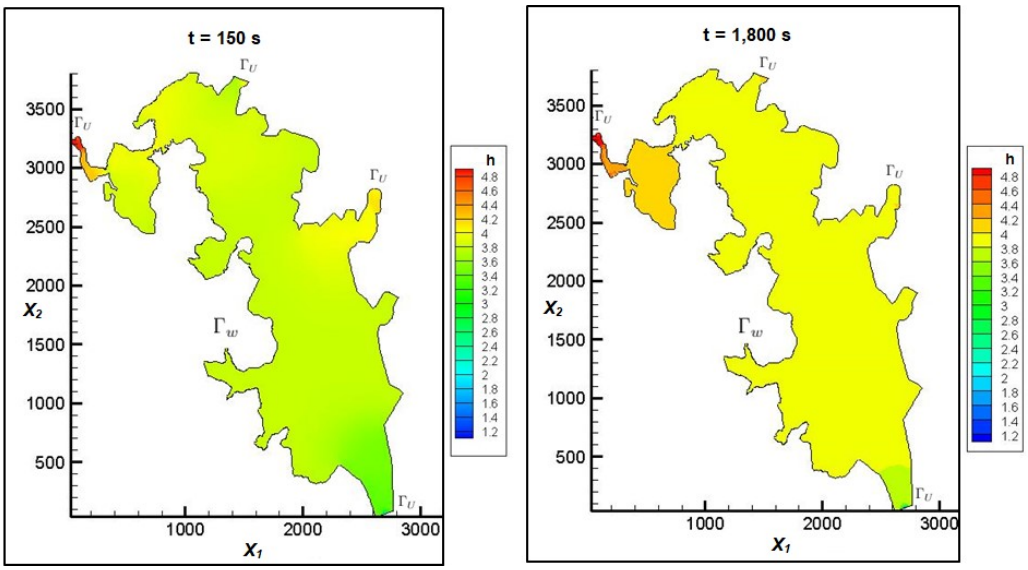

Figure 4. Numerical simulation: a) $t = 150\ s$; b) $t = 1,800\ s$.
Source: authorial.

Following the simulations, in Fig. 5, at $t = 7,200\ s$ and $t = 14,400\ s$ there is an increase in the level of the dam,

with a predominance of the yellow color given by scale. Water has a tendency to remain trapped at the top, due to the geometry, where the highest values of h are still found, now in red $5\ m$, due to the narrowing of the input F. The decrease in the level near the output channel is even more concentrated, decreasing the green area shown in Fig. 4.

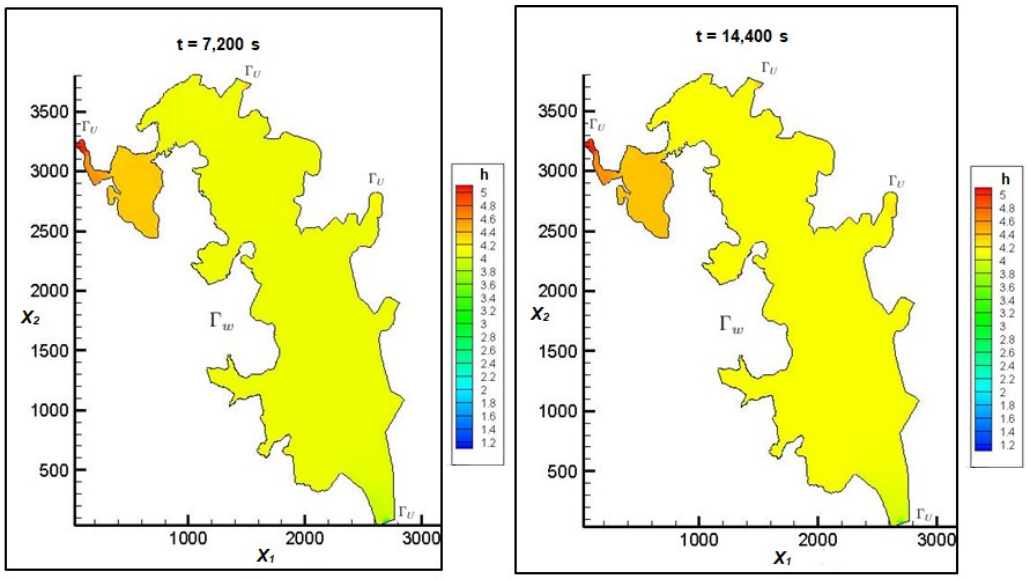

Figure 5. Numerical simulation: a) $t = 7,200\ s$; b) $t = 14,400\ s$.
Source: authorial.

In general, by grading the scale, the level of the dam increases with time, approximately $0.6\ m$ in $14,400\ s$ ($4\ h$) of simulation. Due to the complexity of the geometry of the water resource, the use of triangular finite elements helped to obtain the mesh, making it possible to recognize the highest values of the total water height in the vicinity of channel F, as named in Fig. 3, a very narrow region.

6. CONCLUSION

The numerical simulation in shallow water provides contributions to the understanding of environmental disasters, which can impact on the preservation of human lives and economic damage. This fact occurs because the results obtained provide an approximation about the magnitude of the physical phenomenon, which can be used as a source of information in decision making in front of an event of this nature and its prevention.

The time scheme was used to stabilize the terms of dominant advection, in a totally explicit way. In space, the use of finite triangular elements made it possible to discretize the geometry of the object of study, given its complexity, providing the numerical approximation even in narrow regions.

The simulations shown in Fig. 4 and Fig. 5 show the flow of the dam, with an increase in water level from $3.8\ m$ to $4.4\ m$, approximately, on most of the resource. Over time it is observed that water is retained in the upper part of the dam given the geometry, where the highest total height values are found, in addition to the input contours. And, the lowest levels occur in the vicinity of the Santa Bárbara Channel output contour, concentrating over time.

The behavior observed in Fig. 4 and Fig. 5 occurs in 4 hours (14,400 s), showing the flow given the initial conditions. The simulations characterize the increase in the internal volume of the dam, which can cause inconvenience to the city, since the excess water can cause flooding and even damage to the barrier structure.

Finally, the hydrodynamic modeling presented allows for numerous future perspectives. The mesh can be added to the inhabited areas near the Santa Bárbara Dam, observing the impact of a possible dam break. The shallow water model can be coupled with the optimal control theory and the advection-diffusion equation, restricting the water level by an alternative flow and studying the dispersion of pollutants, respectively.

7. ACKNOWLEDGEMENTS

The authors would like to thank the Municipal Secretariat for City Management and Urban Mobility of Pelotas for providing the topographic data and Coordination for the Improvement of Higher Education Personnel - Brazil (CAPES) for the financial support.

8. REFERENCES

Awruch, A.M., 1983. *Modelos numéricos em hidrodinâmica e fenômenos de transporte usando o método dos elementos finitos*. Ph.D. thesis, Federal University of Rio de Janeiro, Rio de Janeiro, Brazil.

Bukatov, A.E. and Zav'yalov, D.D., 2004. "Wind-induced motion of water in shallow-water closed basins". *Physical Oceanography*, Vol. 14, No. 5, pp. 284 – 294.

Cardoso, F.C.O., 1980. *Um modelo matemático para o controle de poluição das águas*. Master's thesis, Federal University of Rio Grande do Sul, Porto Alegre, Brazil.

Coon, W.F., 1998. *Estimation of roughness coefficients for natural stream channels with vegetated banks*, Vol. 2441. US Geological Survey, New York (USA).

Gill, A.E., 1982. *Atmosphere-Ocean dynamics (International Geophysics Series)*, Vol. 30. Academic Press, London (UK), 2nd edition.

Grave, M., 2016. *Simulação e Controle de Enchentes Usando as Equações de Águas Rasas e a Teoria do Controle Ótimo*. Master's thesis, Federal University of Rio Grande do Sul, Porto Alegre, Brazil.

Huebner, K.H., Dewhirst, D.L., Smith, D.E. and Byrom, T.G., 2001. *Vibration Testing: Theory and Practice*. John Wiley & Sons, New York (USA), 4th edition.

Lima, G.F., 2016. *Avaliação das Áreas de Risco de Inundação no Município de Pelotas, RS: Uma proposta Metodológica*. Graduation thesis, Federal University of Pelotas, Pelotas, Brazil.

Pelotas, P.M., 2016. "Portal de informações geográficas da prefeitura de pelotas". GeoPelotas. 08 Oct. 2020 <geopelotas-pmpel.hub.arcgis.com>.

SANEP, 2020. "Sistema de captação". Serviço Autônomo de Saneamento de Pelotas. 20 Aug. 2020 <portal.sanep.com.br>.

Wijaya, G.B., Bui, T. and Kanok-Nukulchai, W., 2008. "Numerical simulation of tsunami propagation using the characteristic-based split method". *Mathematical Sciences Publishers*, Vol. 3, No. 10, pp. 1939 – 1962.

WINDFINDER, 2020. "Previsão de vento, ondas e tempo: Lagoa dos patos, laranjal". 08 Oct. 2020 <pt.windfinder.com/forecast/lagoa_dos_patos_laranjal>.

Zienkiewicz, O.C., Taylor, R.L. and Nithiarasu, P., 2005. *Finite Element Method for Fluid Dynamics*, Vol. 3. Elsevier: Butterworth-Heinemann.

9. RESPONSIBILITY NOTICE

The authors are solely responsible for the printed material included in this paper.